SECURE LIQUID NITROGEN BACKUP FOR REFRIGERATED BIOSTORAGE

By

Michael Kenworthy Balck

A THESIS

Submitted to
Michigan State University
in partial fulfillment of the requirements
for the degree of

MASTER OF SCIENCE

Mechanical Engineering

2010

ABSTRACT

SECURE LIQUID NITROGEN BACKUP FOR REFRIGERATED BIOSTORAGE

By

Michael Kenworthy Balck

There is need for a secure backup refrigeration system for the long-term storage of biological material. In addition to freezer component failure natural disasters such as Tropical Storm Allison in 2001 in Houston and Hurricane Katrina in 2005 in New Orleans have caused power outages and flooding, leading to the loss of biological specimens when backup refrigeration systems fail. Freezer component failure includes seal leaks, pump and compressor breakdown, and electrical monitoring malfunction. Power outages often result from high winds or large quantities of rain, snow, and ice that disrupt transmission lines. Floodwater, especially from excessive amounts of rain, fills basements and ground floors where biological storage is often located. A non-electrical backup system that can function in the presence of flooding is needed to preserve specimens when the primary system fails.

A liquid nitrogen (LN₂) refrigeration system utilizing a thermostatic expansion valve (TEV) was designed, built, and tested for use as a backup refrigeration system. The non-electric TEV is the key component in the system that can provide secure backup refrigeration for long-term storage of biological specimens. The passive LN₂ refrigeration system does not depend on electricity so it continues to function where common systems fail. Test results of the LN₂ TEV system demonstrated consistent regulation of freezer air temperature within 1°C of the set point. Simulations show that the system's high gain and reserve cooling capacity allows it to hold the temperature steady even during a large increase in ambient temperature.

ACKNOWLEDGMENTS

I would like to thank my advisor, Prof. Clark Radcliffe, for his countless hours of guidance throughout the entire process of this work. Without his help it could not have been finished.

I am also grateful to my family, friends, and colleagues who offered constant support. I am especially appreciative to my parents, Ralph and Nancy, who instilled in me the importance of education and curiosity from an early age. Finally, I would like to offer a special thank you to my wife, Margaret, whose support and encouragement awaited me every night.

TABLE OF CONTENTS

LIST OF TABLES	v
LIST OF FIGURES	vi
LIST OF SYMBOLS	viii
INTRODUCTION	1
LIQUID NITROGEN AS A REFRIGERANT	4
THERMOSTATIC EXPANSION VALVES	8
LN ₂ TEV DESIGN	11
SYSTEM ANALYSIS	15
LINEAR FREEZER CHEST MODEL	18
SENSOR BULB MODEL	22
VALVE ACTUATOR MODEL	23
CONTROL MODEL SIMULATION	24
CONCLUSION	31
APPENDIX A: THERMAL INSULATION CALCULATIONS	34
APPENDIX B : RESISTANCE AND HEAT CAPACITY CALCULATIONS.	35
APPENDIX C : SENSOR BULB HEAT TRANSFER	40
APPENDIX D : HEAT TRANSFER RATES CALCULATION	43
REFERENCES	46

LIST OF TABLES

Table 1. Initial and final nitrogen states during the cooling process	6
Table 2. Component properties [Incropera et al., 2007] and thermal resistance	19
Table 3. Thermal resistances.	20
Table 4. Component material properties [Incropera et al., 2007] and heat capacities	21
Table 5. Resistance and heat capacity summary	39
Table 6. Material properties of copper at 244.5 K [Incropera et al., 2007]	41
Table 7. Thermal properties of air at 244.2 K [Incropera et al., 2007]	41
Table 8. Thermal parameters used in the transient heat transfer rate calculation	44

LIST OF FIGURES

Figure 1. Nearly 50% of the heat absorbed during the cooling process occurs from phase change
Figure 2. Cross section of a thermostatic expansion valve, Parker model N 1/2 JW [Parker Hannifin Corporation, 2007]
Figure 3. Opening and closing forces on the ball bearing at the valve seat
Figure 4. Modified thermal expansion valve for use with LN ₂ (LN ₂ TEV). For interpretation of the references to color in this and all other figures, the reader is referred to the electronic version of this thesis.
Figure 5. The copper seal keeps liquid nitrogen from leaking out of the valve
Figure 6. The seal adapter contains a thin copper membrane
Figure 7. The refrigeration system includes the LN ₂ supply tank, insulated copper tubing, LN ₂ TEV and the freezer chest
Figure 8. Temperature measurements show a rapid decrease and overshoot in air temperature until steady state conditions are reached at about 3500 seconds
Figure 9. LN ₂ TEV refrigeration system feedback control block diagram
Figure 10. LN ₂ TEV refrigeration system heat transfer model
Figure 11. LN ₂ TEV non-linear cooling function with saturation
Figure 12. Simulated freezer air temperature matches the steady state experimental values and captures the qualitative transient behavior
Figure 13. The simulated sensor bulb temperature decreases slower than experimental measurements but matches the steady state values
Figure 14. The simulation predicts the qualitative behavior of the valve as well as the correct steady state heat transfer rate.
Figure 15. Timing and overshoot is improved with alterations to the model while steady state behavior is not significantly changed

Figure 16. Simulation shows that the LN ₂ TEV system is well suited to b refrigeration system during the worst conditions of a power failure	
Figure 17. Chest interior dimensions.	35
Figure 18. Chest exterior dimensions.	36
Figure 19. Chest insulation dimensions.	37
Figure 20. Sensor bulb geometry.	40

LIST OF SYMBOLS

A	Area
С	Heat capacity
c	Specific heat capacity
E	Thermal energy
Ė	Time rate of change of thermal energy
h	Convection heat transfer coefficient
k	Thermal conductivity
l	Length
\dot{m}	Mass flow rate
Q	Heat transfer
\dot{Q}	Heat transfer rate
q	Specific heat transfer
R	Thermal resistance
T	Temperature
\dot{T}	Time rate of change of temperature
V	Volume
ρ	Density
τ	Time constant
COP	Coefficient of performance
LN_2	Liquid nitrogen
TEV	Thermostatic expansion valve

INTRODUCTION

Biostorage is growing in importance for medical and biological research. *Biostorage* is the preservation of biological material in a temperature controlled environment. An example of biostorage is the Archive for Research on Child Health (ARCH) project at the College of Human Medicine at Michigan State University managed by the Institute for Health Care Studies (IHCS). The purpose of the project is to connect "...the collection of biological specimens from Michigan newborns to medical and vital records and allows for scientific investigation and research on pregnancy and childhood health conditions" [Institute for Health Care Studies, 2010]. To do this, the original samples must be carefully stored to protect their integrity for many decades. Furthermore, the individual is periodically tested, with the results being recorded and added to a file containing all previous test results. The initial samples and all test results become more valuable as time passes because the amount of data increases.

Severe weather resulted in the loss of thousands of biological samples, costing millions of dollars and years of research. In 2001 "...cancer, AIDS and other medical research was lost when power to freezers failed and cell cultures were destroyed" in Baylor College of Medicine laboratories during Tropical Storm Allison [Turner, et al., 2001]. Hurricane Katrina in 2005 affected about 300 federally funded projects at colleges and universities in New Orleans according to a survey conducted by the National Institutes of Health [Associated Press, 2005]. Frozen blood and urine samples from thousands of donors were destroyed when electricity was lost followed by the failure of backup generators at Tulane University [Associated Press, 2005].

Existing freezer backup systems are not reliable enough for long-term storage. They fail in many ways including malfunction of mechanical and electrical components, power loss, and flooding. Any one of these failures can lead to the destruction of biological samples. Flooding and power loss often happen concurrently during large storms.

Complex machinery and electronics in freezers can fail over time. Seals, bearings, electrical connections, and system batteries can all deteriorate. A common backup for this type of failure is a second, stand alone system. This system is just as complex, expensive, and unreliable as the system it replaces.

Existing backup systems require a second source of electrical power when a power outage occurs. This second source can either be a gas powered generator or a battery. The generator is used to power the mechanical refrigeration system and electrical controls. A generator is vulnerable to flooding and requires a large supply of fuel to power a collection of low temperature freezers. Batteries are used to run electronic controls for the release of liquid carbon dioxide or nitrogen. These systems have limited amounts of refrigerant on hand. Also, batteries are not a reliable source of power. According to a freezer manufacturer's technical bulletin, batteries "...can develop a memory which can severely limit the reserve capacity when needed the most" [Sanyo, 2010]. Manufacturers recommend that these batteries be replaced approximately every three years regardless of their condition [Sanyo, 2010] adding an expensive, time consuming, and difficult to manage task to facility management.

Flooding is often the cause for system failures. Floodwater shorts electrical controls and motors driving compressors and pumps that are often located close to floors due to their weight. Water can also infiltrate generators and cause electrical failure of secondary power sources. Non-electrical failure due to flooding includes damage to bearings and drive belts. If allowed to contact specimens, floodwater can compromise their integrity.

A robust backup system would have reliable and simple components, be non-electrical, flood resistant, and able to run for an extended period. The LN₂ TEV backup system meets all of these criteria. The LN₂ TEV has simple, low force mechanics for increased reliability. The system is thermodynamically driven so electrical power is not needed and floodwaters do no harm. Finally, most medical research facilities have large stores of LN₂ on site so the backup system can be easily installed and run for an extended period.

The process of designing a reliable backup refrigeration system was motivated by the consequences of using LN₂ as the refrigerant with a TEV as the regulator. The first step was determining the cooling ability of LN₂. Next was researching how TEVs normally operate and how LN₂ temperatures affect their performance. Finally was the design and implementation of solutions for the problems caused by low temperatures with the TEV.

LIQUID NITROGEN AS A REFRIGERANT

Nitrogen is a plentiful and non-toxic gas. It makes up 78% of earth's atmosphere by mole fraction [Moran and Shapiro, 2004]. Commercially, LN₂ is a byproduct of the production of liquid oxygen. It is a very inexpensive liquid at 20 cents per gallon in bulk because it is so plentiful [Radcliffe, 2007]. Liquid nitrogen is stored in large tanks at a pressure of 22 psig (36.7 psia) and a temperature of -187°C. It can be used as a refrigerant and has the designation R-728. A refrigerant is a substance that is used to transfer thermal energy from one space to another. Fluids that are able to absorb and release large amounts of energy corresponding to phase changes are often used as refrigerants.

Liquid nitrogen cools a space or object by absorbing energy from it in a complex process involving boiling and temperature change. The three steps of cooling can be seen in (Fig. 1), which shows the amount of energy that is absorbed by the nitrogen during the cooling process. The process will be described by following the heat absorbed along the 36.7 psia (22 psig) line. In the first step, liquid nitrogen warms until it reaches its boiling point. This corresponds to a movement from point A to point B. Next the liquid nitrogen boils at constant temperature until it is entirely gas phase, going from point B to point C. Finally the nitrogen gas warms until it reaches an equilibrium temperature with its surroundings as there is movement from point C to point D. Heat energy is transferred from the surroundings to the nitrogen in each step.

The cooling process involved in the LN_2 TEV backup refrigeration system differs in two ways from that shown in (Fig. 1). The LN_2 is delivered in a pressure regulated tank so the initial temperature of the LN_2 is forced to be the boiling point at 36.7 psia (22 psig) because the liquid continuously boils due to the tank's warm environment. The temperature of the nitrogen must be -187° C because pressure regulator forces the pressure to be 36.7 psia (22psig). Gauge pressure,

Heat Absorbed During LN₂ Cooling Process 450 F 400 Heat Absorbed (kJ/kg) 350 Gas, Phase D 300 250 14.7 psi 200 $\overline{\mathbf{C}}$ 36.7 psi 150 Phase Change 100 50 Liquid Phase -200 -175 -150 -125-100 -75 -50 -25 0 25 Final Nitrogen Temperature (°C)

Figure 1. Nearly 50% of the heat absorbed during the cooling process occurs from phase change.

psig, is referenced to standard atmospheric absolute pressure, 14.7 psia. The state 36.7 psia and -187°C corresponds to point B. The second difference is that there a pressure drop as the liquid is released through the LN₂ TEV orifice. As the LN₂ passes through the TEV orifice, the nitrogen's pressure changes from 36.7 psia to 14.7 psia yielding rapid boiling and phase change from liquid to gas. The TEV causes the nitrogen to move between points B and E. The state of the LN₂ lies on the vertical portion of the dashed 14.7 psia line as the mixed phase nitrogen boils completely. Once it is completely gas phase, the nitrogen gas warms and the state moves from point E to point F along the 14.7 psia line.

The amount of energy absorbed per unit mass q_{LN2} from the surroundings depends on nitrogen's the latent heat of vaporization h_{fg} at the boiling temperature T_{BP} , its specific heat capacity c_{LN2} , and the final temperature T_{eq} (1).

$$q_{LN2} = h_{fg} + (T_{eq} - T_{BP})c_{LN2} \tag{1}$$

Liquid nitrogen absorbs 199 (kJ/kg) to boil to a gas at 14.7 psia and constant temperature. Once the nitrogen is in gas phase it continues to absorb heat at a rate of 1.048 (kJ/kg-°C), its average specific heat during the temperature rise, until an equilibrium temperature is reached. The initial state of the LN₂ in the LN₂ TEV backup refrigeration system is defined by a pressure of 36.7 psia (22 psig) and a temperature of -187°C. The final state is atmospheric pressure, 14.7 psia, and -29°C. The temperature rise of the nitrogen gas is 167°C yielding a heat absorption value of 175 (kJ/kg). The total heat absorption of the nitrogen is the 374 (kJ/kg) (2).

$$q_{LN2} = 199 \left(\frac{\text{kJ}}{\text{kg}}\right) + \left[-29^{\circ}\text{C} - (-196^{\circ}\text{C})\right] \times 1.048 \left(\frac{\text{kJ}}{\text{kg} \cdot ^{\circ}\text{C}}\right) = 374 \left(\frac{\text{kJ}}{\text{kg}}\right)$$
 (2)

Another method of determining the energy absorbed by the nitrogen is to look at its initial and final energy states defined by enthalpy (Table 1). The total heat absorbed by the nitrogen is equal to the difference in the enthalpies of the initial and final states. In this case the heat absorbed is 362 (kJ/kg), which is very close to the calculation done earlier. A value of 360 (kJ/kg) will be used for the heat absorption.

Table 1. Initial and final nitrogen states during the cooling process [Reynolds, 1979]

[110]110100, 12,73								
State	Phase	Temperature (°C)	Pressure (psia)	Enthalpy (kJ/kg)				
Initial	Liquid	-187	36.7	43				
Final	Vapor	-27	14.7	405				

The cost of cooling with LN_2 can be compared to cooling with electricity in the form of dollars per kilo-Joule of cooling [Radcliffe, 2007]. The heat absorption of LN_2 in kilo-Joules per kilogram can be converted to kilowatt-hours per gallon using the density of LN_2 and unit conversion (3).

$$360 \left(\frac{\text{kJ}}{\text{kg}}\right) \times 3.07 \left(\frac{\text{kg}}{\text{gallon}}\right) \times 2.78 \times 10^{-4} \left(\frac{\text{kW-hr}}{\text{kJ}}\right) = 0.31 \left(\frac{\text{kW-hr}}{\text{gallon}}\right)$$
(3)

Liquid nitrogen costs about 20 cents per gallon in bulk [Radcliffe, 2007] resulting in the cost of cooling with LN_2 to be 65.1 (cents/kW-hr) (4).

$$20\left(\frac{cents}{gallon}\right) \div 0.31\left(\frac{kW-hr}{gallon}\right) = 65\left(\frac{cents}{kW-hr}\right) \tag{4}$$

The retail cost of electricity for commercial use in Michigan is 10.11 (cents/kW-hr) [U.S. Energy Information Administration, 2010]. Heat pumps, such as refrigerators and freezers, are known to have a coefficient of performance (COP) of about 2.5 [Radermacher et al., 2007]. This means that they provide 2.5 times the amount of cooling energy as they use in electrical energy. Therefore the cost of cooling with electricity is about 4 cents per kW-hr. The cost of cooling with LN₂ is about 16 times greater than using electricity. A LN₂ refrigeration system is not intended as a primary system because of this cost. However, when an electrical power outage occurs it is well worth the cost to use a LN₂ backup refrigeration system to preserve biological specimens.

THERMOSTATIC EXPANSION VALVES

Thermostatic expansion valves (TEVs) are flow controlling devices that operate according to the temperature they sense. They are found in many commercial refrigeration and air conditioning systems including walk-in-coolers, beverage dispensers, and ice machines [Parker Hannifin Corporation, 2007]. A TEV is installed between the compressor and evaporator in normal refrigeration systems. In the LN₂ backup refrigeration system the TEV is connected to the refrigerant supply line and is located in the freezer chest which acts as the evaporator. TEVs control the cooling process and adjust the freezer temperature by regulating the flow of refrigerant.

TEVs (Fig. 2) operate by sensing the temperature of the space it is cooling, actuating flow regulation, and providing flow area expansion and pressure drop. When the TEV senses that the space is too warm, refrigerant is allowed to flow to cool the space. When the TEV senses that the space is too cold The TEV stops the flow of refrigerant, allowing the space to warm up. The process repeats when the object again becomes too warm.

The TEV senses temperature by a thermodynamic process within the TEV's sensor bulb. The sensor bulb is made of copper and contains a refrigerant charge that reacts to the temperature it is sensing. The charge boils and expands when the bulb becomes warmer than its set point. A large pressure rise results from the phase change since limited volume is available. When the temperature is below the set point, the charge condenses, which results in a low pressure. The actuator reacts to this pressure signal.

The TEV's actuator is a thin, flexible, metal diaphragm. The top side of the diaphragm is open to the refrigerant charge in the sensor bulb. A small copper capillary tube allows the flow of the charge between the sensor bulb and the top side of the diaphragm. The other side of the

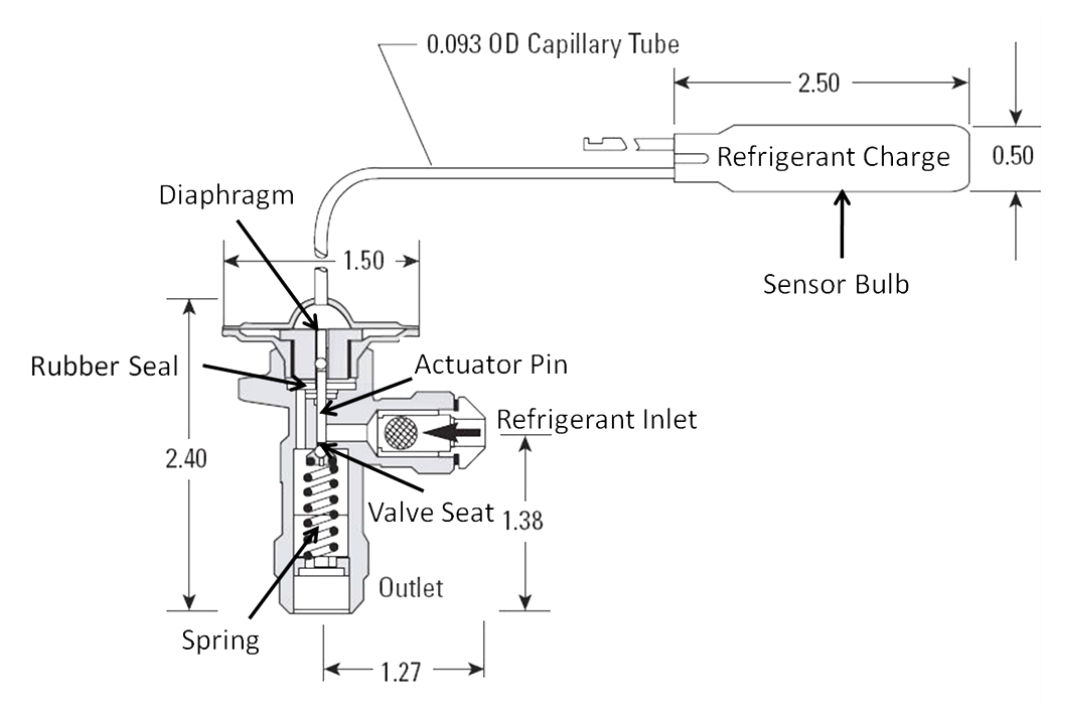


Figure 2. Cross section of a thermostatic expansion valve, Parker model N 1/2 JW [Parker Hannifin Corporation, 2007]

diaphragm is connected to a ball bearing in the valve seat through an assembly containing an actuator pin. The diaphragm transmits a downward force on the ball bearing which acts to allow the flow of refrigerant. The force transmitted by the diaphragm increases with rising pressure in the sensor bulb.

A spring is used to counteract the opening force. The spring is located below the valve seat and acts to push the ball bearing into the seat to stop the flow of refrigerant. The spring is supported by a nut that rides inside the valve's outlet. The nut can be turned to vary the spring's preload which adjusts the TEV's temperature set point.

The TEV set point is determined by the balance of the opening and closing forces (Fig. 3). The opening forces include the refrigerant charge pressure acting on the diaphragm area and the refrigerant gauge pressure acting on valve orifice area. The latter force is negligible since the pressure is relatively low and the orifice is relatively small. The closing force is the

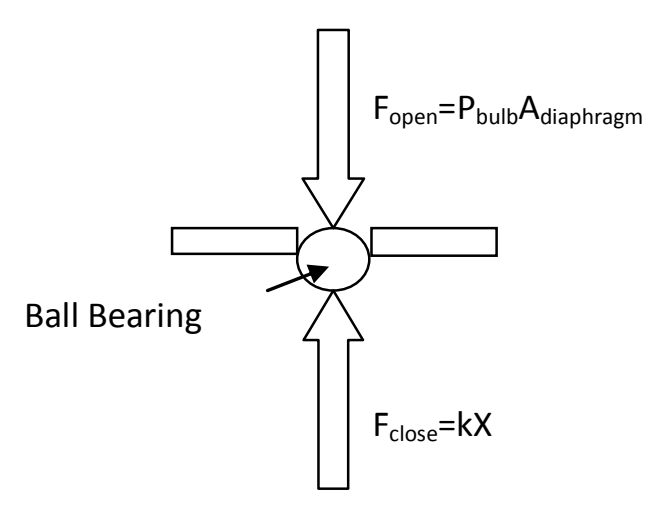


Figure 3. Opening and closing forces on the ball bearing at the valve seat.

spring force. The set point temperature is the temperature at which the force created by the bulb pressure exactly matches the spring force in a closed position. For the Parker N 1/2 JW TEV this temperature was measured to be -30°C. If the bulb temperature rises above the set point a corresponding pressure rise occurs that overcomes the spring force and pushes the ball bearing off the valve seat. Refrigerant is then free to flow and cool the space.

LN₂ TEV DESIGN

Problems occur when using a conventional TEV with LN₂ as the refrigerant. The very low temperature of LN₂ causes the rubber seal (Fig. 2) around the actuator pin to harden and deform and could cause the refrigerant charge to freeze. The hardened and deformed rubber seal allows the LN₂ to leak to the underside of the diaphragm and also impedes the motion of the actuator pin. The seal holds the actuator pin in the open position which allows constant flow of LN₂ into the freezer chest while the freezer air and valve temperatures drop to well below -150°C. The refrigerant charge on the topside of the diaphragm and in the bulb quickly condenses and is believed to freeze. Its freezing temperature is believed to be close to -100°C. This is approximately the freezing temperature of R-134a [Air Liquide, 2009], one of the conventional refrigerants used with this TEV. TEV charges and the refrigerants used with them have similar thermodynamic properties. A frozen charge would not allow the diaphragm to move and would not flow between the diaphragm and sensor bulb.

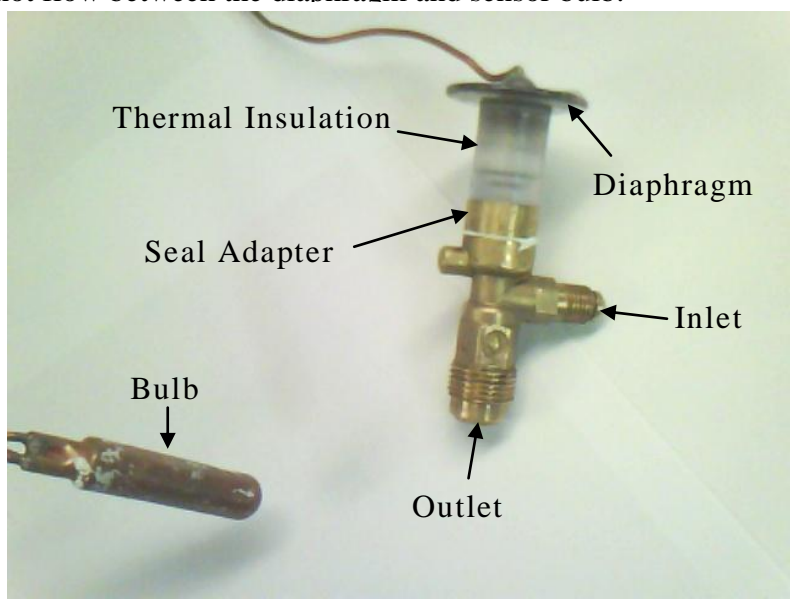


Figure 4. Modified thermal expansion valve for use with LN₂ (LN₂ TEV). For interpretation of the references to color in this and all other figures, the reader is referred to the electronic version of this thesis.

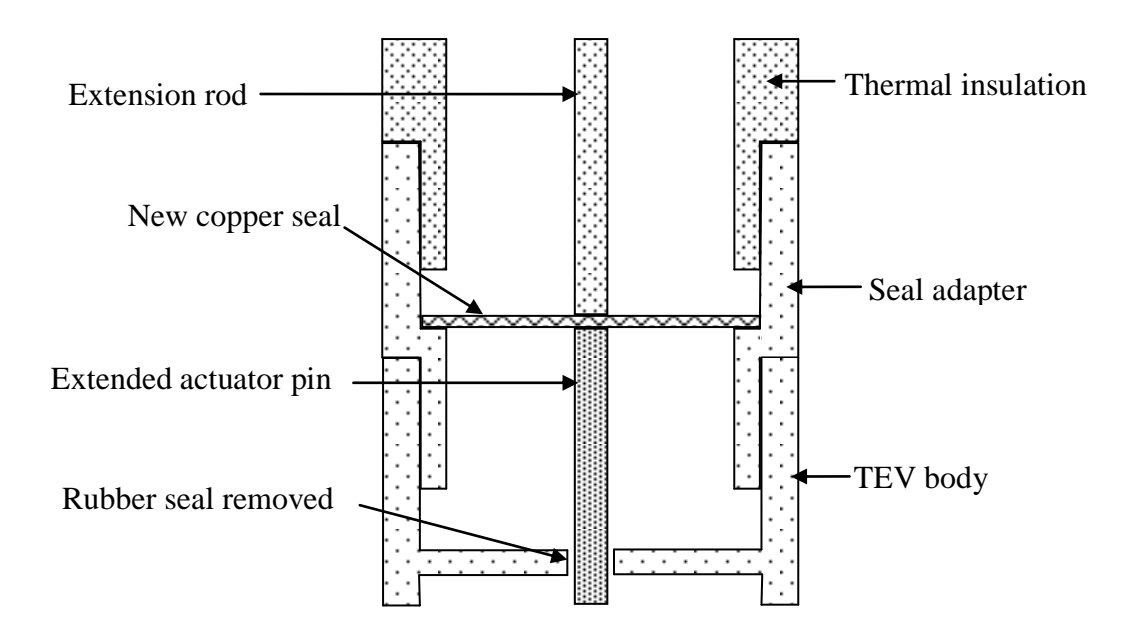


Figure 5. The copper seal keeps liquid nitrogen from leaking out of the valve.

Two modifications were made to the TEV design to allow it to be used with LN_2 (Fig. 4). The rubber seal was removed and a new seal was installed to keep the liquid nitrogen from leaking. The actuator pin had to be lengthened to accommodate the new seal. Then thermal insulation was inserted between the valve body and the diaphragm to keep the refrigerant charge from freezing.

A thin copper membrane was placed between the actuator pin and the thermal insulation extension to prevent LN₂ from leaking out of the valve (Fig. 5). Copper was used for the seal because it does not become deformed or harden like rubber does at LN₂ temperature. Corrugations were pressed into the membrane to ensure that the seal would have enough flexibility to move without breaking. The copper seal (Fig. 6) was fabricated from 0.001" copper shim stock and has a diameter of 0.5". The copper membrane was soldered into a brass adapter. The brass adapter was fabricated to easily screw into both the valve body and thermal insulation.



Figure 6. The seal adapter contains a thin copper membrane.

The second modification was placing thermal insulation between the diaphragm and the valve body to keep the refrigerant charge from freezing. The insulation is a polycarbonate cylinder that connects the diaphragm to the valve body while a polycarbonate extension rod links the copper membrane and the diaphragm. Thermal insulation design balanced the conductive heat transfer from the diaphragm to the valve body with the convective heat transfer from the freezer air to the diaphragm. The goal was to make the insulation length long enough to keep the diaphragm above -100°C, the suspected highest freezing temperature of the refrigerant charge. The length was calculated to be 2.6 cm using a factor of safety of 2 [App. A]. The force needed to buckle the extension rod was then calculated to be 410 N [App. A], much greater than the forces involved with valve operation.

The LN_2 TEV system is capable of running under flood conditions. If water breaches chest seals it will freeze upon coming into contact with the -25°C interior chest walls which helps to further seal the chest. Also the chest is pressurized to 22 psig from the LN_2

supply tank. For water to overcome this pressure and force itself into the bottom of the chest it would have to be over 50 ft deep. Meanwhile, the TEV would continue to supply the chest with LN_2 .

SYSTEM ANALYSIS

Mathematical models were developed to analyze the system, explain system behavior, and predict system response to a power failure and rise in ambient temperature. First a linear model for the heat transfer between the freezer chest and the surrounding environment was developed. Then another heat transfer model was developed to describe the sensor bulb. Next a nonlinear model was used to explain the action of the thermostatic expansion valve. Finally, a control model was produced to predict system response.

The refrigeration system consists of the LN_2 supply tank, insulated copper tubing, LN_2 TEV, and the freezer chest (Fig. 7). The freezer is considered as a rectangular chest with

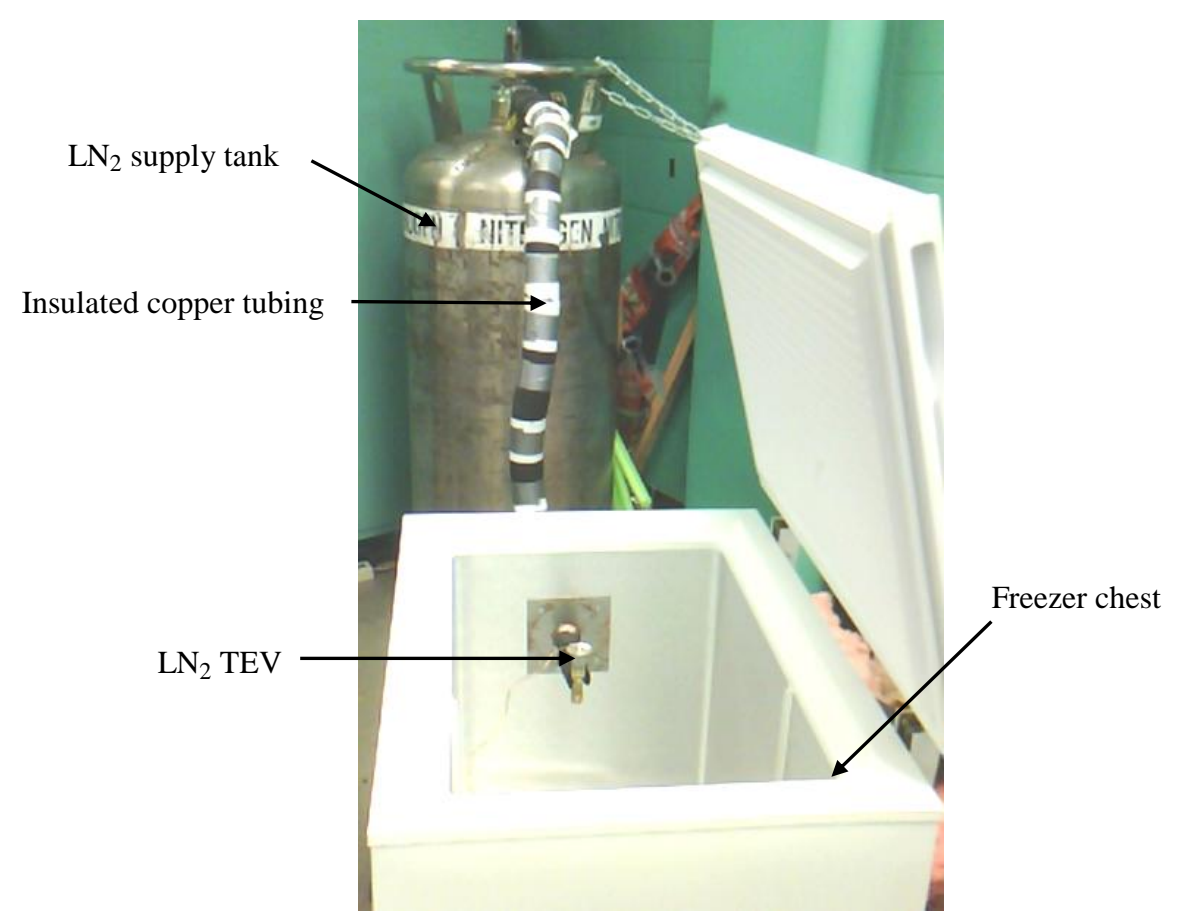


Figure 7. The refrigeration system includes the LN_2 supply tank, insulated copper tubing, LN_2 TEV and the freezer chest.

insulated walls. The chest walls and bottom are made of two thin aluminum (Al) sheets with a thick layer of urethane foam insulation in between. The interior chest ceiling is made of polystyrene (PS). The nitrogen is dispensed from the TEV, which is suspended in the middle of the chest. Operating at room temperature (24°C), a heavily insulated, small diameter, copper tube connects the TEV to the LN₂ supply tank outside the chest.

Experiments were run to gain understanding of the system. Thermocouples were placed in the freezer air, on the sensor bulb, interior wall, exterior wall, and in the room outside of the chest to track their temperatures throughout the experiment (Fig. 8). The chest air and bulb temperature reach steady state at about 3500 seconds and a temperature of -29°C. The interior wall and exterior wall reach steady state temperatures of -24.5°C and 22.2°C respectively. The room temperature stays near 24°C.

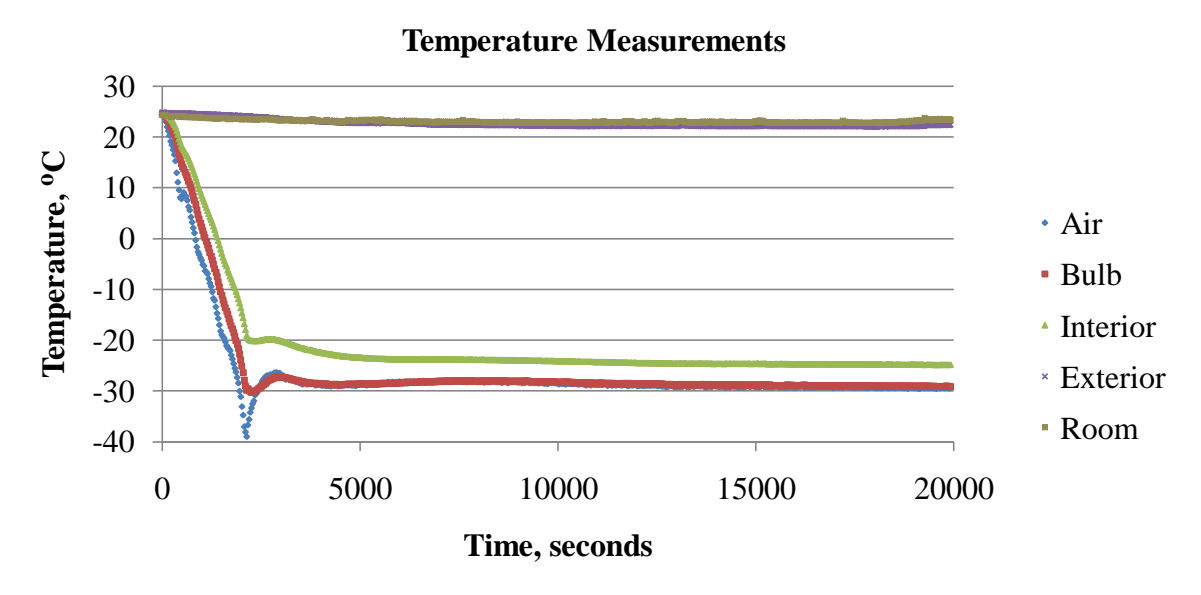


Figure 8. Temperature measurements show a rapid decrease and overshoot in air temperature until steady state conditions are reached at about 3500 seconds.

The LN₂ TEV refrigeration control system consists of three major components; freezer chest, sensor bulb, and valve actuator (Fig. 9). The heat transfer rate \dot{Q}_{LN2} and room temperature T_{room} are inputs to the freezer chest. The result is the air temperature inside the chest, T_{air} . T_{bulb} is the sensor bulb measurement of T_{air} . T_{bulb} determines the pressure inside the bulb that acts upon the diaphragm. This pressure acts against the set point temperature, T_{set} , also expressed physically as the pressure resulting from the spring's preload force. The difference between T_{set} and T_{bulb} is the system error. The valve actuator responds to the system error by opening and releasing LN₂ or shutting off the LN₂ flow. If the error is negative the pressure in the bulb is great enough to displace the spring. This corresponds to a measured temperature that is warmer than the set point temperature. A negative error causes the release of LN₂ and heat absorption to occur inside the chest. A positive or zero error will result in the valve closing and no release of nitrogen. Physically this means that the closing spring force is greater than the opening force caused by the bulb pressure.

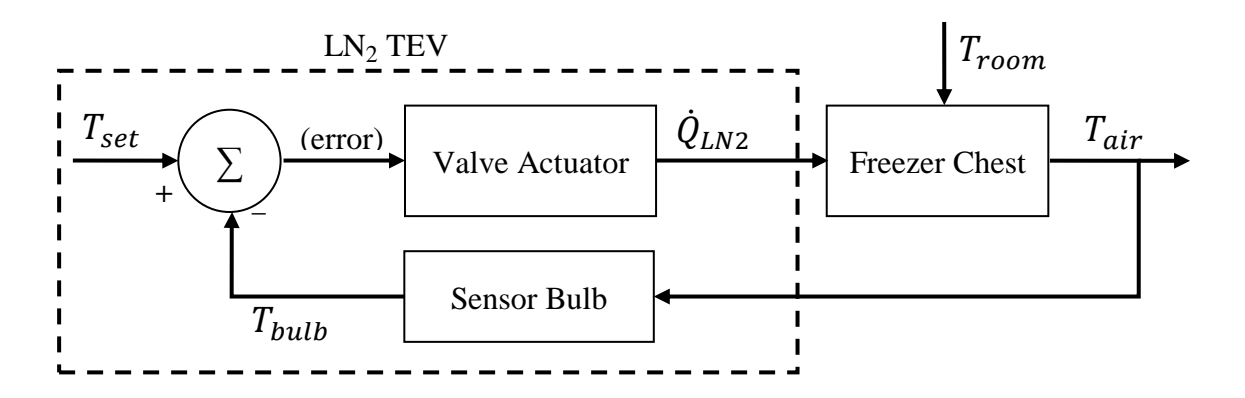


Figure 9. LN₂ TEV refrigeration system feedback control block diagram.

LINEAR FREEZER CHEST MODEL

The freezer chest was separated into four thermal masses for the mathematical model; exterior wall, foam insulation, interior wall, and freezer air (Fig. 10). Each of these components has a thermal energy E related to a temperature T. There is a thermal resistance R associated with the heat transfer rate \dot{Q} between each component. There is a heat transfer rate into the system from the room and the heat transfer rate out of system from the heat absorbed by LN₂. The model has four thermal states (T_{air} , T_{int} , T_{ins} , T_{ext}), two inputs (T_{room} , \dot{Q}_{LN2}), and one output (T_{air}).

The heat transfer model for each mass is derived from an energy balance. According to conservation of energy, each mass's time rate of change of energy

$$\dot{E}_{mass} = \sum \dot{Q}_i \tag{5}$$

where \dot{Q}_i are the heat transfer rates into, and out of, the associated mass. The heat transfer rate between components of the freezer chest

$$\dot{Q} = \frac{1}{R} (T_{hot} - T_{cold}) \tag{6}$$

is driven by the temperature difference between the components and inversely related to the

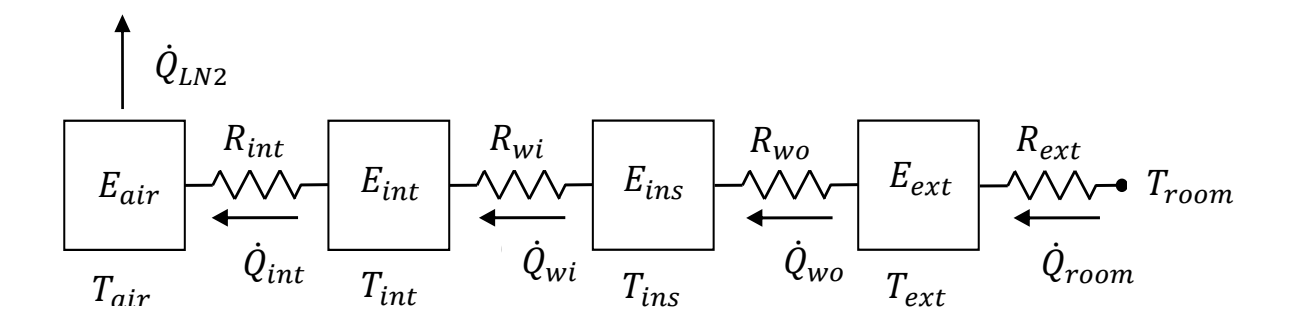


Figure 10. LN₂ TEV refrigeration system heat transfer model.

thermal resistance between the hot and cold components.

The values of the thermal resistances R_{wi} and R_{wo} were calculated using physical measurements of the system components and material properties taken at steady state temperatures. The location of the insulation temperature T_{ins} was chosen such that the interior wall resistance R_{wi} and the exterior wall resistance R_{wo} are equal to each other and one half of the total resistance between the interior wall temperature T_{int} and the exterior wall temperature T_{ext} . The total resistance of the composite wall R_{total} is the sum of the resistances of the two aluminum sheets and the foam insulation. Each resistance is calculated [App. B] using (7), where k is the thermal conductivity of the material, l is the thickness of the material, and A is the conduction area (Table 2).

$$R = (1)/(kA) \tag{7}$$

Table 2. Component properties [Incropera et al., 2007] and thermal resistance

Component	Thermal Conductivity k (W/m-K)	Thickness l (m)	Area A (m^2)	Resistance R (K/W)
Exterior Wall (Al)	176	7.5x10 ⁻⁴	2.76	1.5x10 ⁻⁶
Foam Insulation	0.04	$7.0 \text{x} 10^{-2}$	2.35	1.2
Interior Wall (Al) Interior Wall (PS)	170 0.13	7.5x10 ⁻⁴	1.45 0.25	3.0x10 ⁻⁶

The total resistance of the wall

$$R_{total} = 1.5 \times 10^{-6} \left(\frac{K}{W}\right) + 1.2 \left(\frac{K}{W}\right) + 3.0 \times 10^{-6} \left(\frac{K}{W}\right) = 1.2 \left(\frac{K}{W}\right)$$
 (8)

The foam insulation's low heat transfer coefficient accounts for most of the resistance of the wall. The value of R_{wi} and R_{wo} is then 0.6 (K/W).

The system is at steady state when temperatures cease to change. This corresponds to each mass reaching a constant energy. If a mass is at a constant energy then the heat transfer rate into the mass is equal to the heat transfer rate out of the mass. This implies that each heat transfer rate is equal to one another at steady state. The value of the steady state heat transfer rate is most accurately calculated using the calculated total wall resistance and measured steady state temperatures of the exterior wall T_{ext} and interior wall T_{int} (9).

$$\dot{Q}_{ss} = [295.4 (K) - 248.7 (K)]/1.2 (K/W) = 39 (W)$$
 (9)

The interior resistance R_{int} between the interior wall and freezer air, and exterior resistance R_{ext} , between the exterior wall and room air, were calculated (Table 3) using temperature measurements, the calculated steady state heat transfer rate, and (9).

Table 3. Thermal resistances

R _{int}	R_{wi}	R_{ext}		
0.12 (K/W)	0.6 (K/W)	0.6 (K/W)	0.018 (K/W)	

The energy stored in a freezer component is a function of the component's temperature and heat capacity C. The component's heat capacity is the product of its specific heat capacity and mass. The time rate of change of energy stored in the component is dependent on the time rate of change of the component's temperature (10).

$$\dot{E}_{stored} = C\dot{T} \tag{10}$$

Heat capacities (Table 4) were calculated [App. B] using physical measurements for the material volume and the material properties of density and specific heat capacity (11).

$$C = V\rho c \tag{11}$$

Table 4. Com	ponent	materia	i pro	perties	Incro	pera et al.,	2007	and	neat	ca	pacities
	T 7 1	T 7	ъ	•					_		0

Component	Volume V (m^3)	Density ρ (kg/m ³)	Specific Heat C (J/kg-K)	Heat Capacity <i>C</i> (J/K)
Air	0.14	1.4354	1006	2.0×10^2
Interior (Al) Interior (PS)	1.1 x 10 ⁻³ 1.9 x 10 ⁻⁴	2770 1050	830 1170	2.7×10^3
Insulation	0.16	70	1045	1.2×10^4
Exterior	2.1×10^{-3}	2770	871	5.1×10^3

The heat transfer model is assembled by applying (6) and (10) to (5) for each freezer component and dividing through by the heat capacity (12a-d).

$$\dot{T}_{air} = (1/C_{air})[(1/R_{int})(T_{int} - T_{air}) - \dot{Q}_{LN2}]$$
(12a)

$$\dot{T}_{int} = (1/C_{int})[(1/R_{wi})(T_{ins} - T_{int}) - (1/R_{int})(T_{int} - T_{air})]$$
(12b)

$$\dot{T}_{ins} = (1/C_{ins})[(1/R_{wo})(T_{ext} - T_{ins}) - (1/R_{wi})(T_{ins} - T_{int})]$$
(12c)

$$\dot{T}_{ext} = (1/C_{ext})[(1/R_{ext})(T_{room} - T_{ext}) - (1/R_{wo})(T_{ext} - T_{ins})]$$
(12d)

The model can then be filled in with the calculated values for the thermal resistances and heat capacities (13a-b).

$$\dot{T}_{air} = (1/2.0 \times 10^2) [(1/0.12)(T_{int} - T_{air}) - \dot{Q}_{LN2}]$$
(13a)

$$\dot{T}_{int} = (1/2.7 \times 10^3)[(1/0.6)(T_{ins} - T_{int}) - (1/0.12)(T_{int} - T_{air})]$$
 (13b)

$$\dot{T}_{ins} = (1/1.2 \times 10^4) [(1/0.6)(T_{ext} - T_{ins}) - (1/0.6)(T_{ins} - T_{int})]$$
(13c)

$$\dot{T}_{ext} = (1/5.1 \times 10^3)[(1/0.018)(T_{room} - T_{ext}) - (1/0.6)(T_{ext} - T_{ins})] \quad (13d)$$

The above model can be written in matrix form, $\dot{T} = AT + Bu$, where T is the state vector, u is the input vector, and the matrices A and B are given in (14) and (15) respectively.

$$\mathbf{A} = 10^{-3} \times \begin{bmatrix} -41.7 & 41.7 & 0 & 0\\ 3.1 & -3.7 & 0.6 & 0\\ 0 & 0.1 & -0.3 & 0.1\\ 0 & 0 & 0.3 & -11.2 \end{bmatrix}$$
(14)

The output equation (16) yields T_{air} .

$$Y = [1 \quad 0 \quad 0 \quad 0]T \tag{16}$$

SENSOR BULB MODEL

The sensor bulb is a copper cylinder that contains a refrigerant charge. Broersen [1982] has investigated the bulb time constant τ_{bulb} . During normal use, the bulb's time constant can be as short as 16.2 seconds for tightly clamped and as long as 60 seconds for loosely attached to the refrigerant tubing of an evaporator. In the LN₂ TEV application, the bulb is suspended in open air and relies on natural convection for heat transfer causing the time constant to be much longer.

The heat transfer dynamic model of the sensor bulb is assembled in the same manner as the previous heat transfer models (17).

$$\dot{T}_{bulb} = (1/\tau_{bulb})(T_{air} - T_{bulb}) \tag{17}$$

The bulb time constant $\tau_{bulb} = mc/hA = 1100$ seconds [App. C], over 18 times longer than when attached mechanically. The sensor bulb model can be written in matrix form (18-19).

$$\dot{T}_{bulb} = [-1/1100]T_{bulb} + [1/1100]T_{air} \tag{18}$$

$$y = [1]T_{bulb} \tag{19}$$

VALVE ACTUATOR MODEL

The valve actuator takes the measured temperature error, T_{set} - T_{bulb} , and converts it to a heat transfer rate. The system acts to minimize the temperature error by regulating the heat transfer rate out of the freezer. Physically it does this by regulating the orifice area at the valve seat. The area and pressure drop across the orifice are factors that determine the mass flow rate of LN_2 \dot{m}_{LN2} . The heat transfer rate out of the freezer

$$\dot{Q}_{LN2} = q_{LN2} \times \dot{m}_{LN2} \tag{20}$$

The valve actuator applies a cooling function to the system (Fig. 11). Saturation of \dot{Q}_{LN2} occurs because a maximum flow area is reached. The cooling function is linear for small errors with a slope of -40 (W/°C) and saturates at \dot{Q}_{LN2}^{Sat} equal to 100 (W) for errors below -2.5°C and at 0 (W) for errors at or above 0°C. The steady state operating point occurs at an error of -1°C and 40 (W). The saturation limit of 100 (W) was determined from experimental data and (13a) [App. D]. The air temperature has an average slope of -0.029 (K/s) during the transient and the average value of $(T_{int} - T_{air})$ is 12 (K). Using these values with (13a) gives a maximum value of 100 (W) for \dot{Q}_{LN2} . The set point was determined to be -30°C by measuring the temperature at which the valve starts to open. The steady state temperature is approximately -29°C which gives a steady state error of -1°C and steady state heat transfer rate of 40 (W). A linear interpolation of the points [0°C error, 0 (W)] and [-1°C error, 40 (W)] gives a slope of -40 (W/°C).

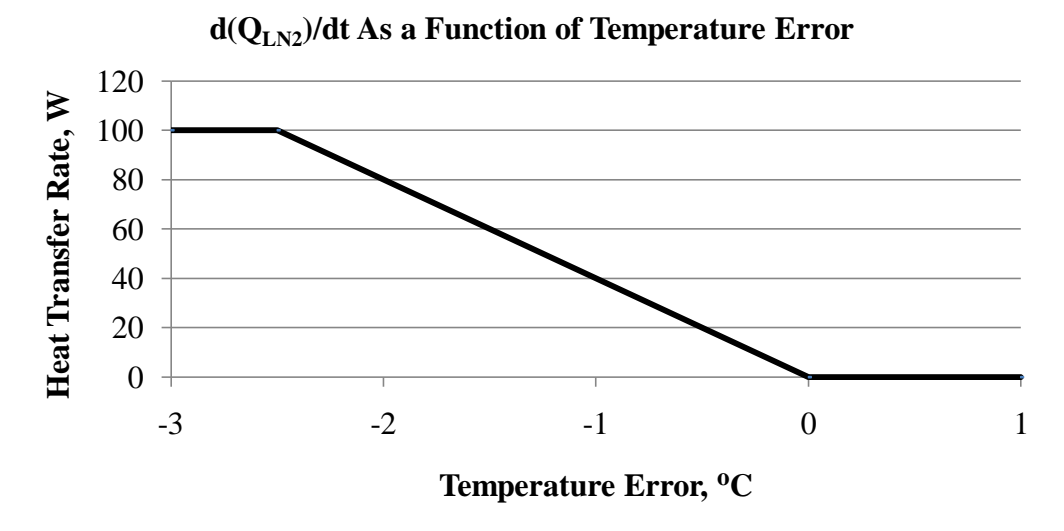


Figure 11. LN₂ TEV non-linear cooling function with saturation.

CONTROL MODEL SIMULATION

Simulation of the control model yields results close to the experimental data (Fig. 12). The difference in the transient behavior can be attributed to the linear thermal model of the freezer chest. The model is valid for small variations about the operating point. The transient covers a temperature change of over 60°C which leads to inaccurate assumptions for material properties and convective heat transfer coefficients. The model does predict the qualitative behavior of the freezer that includes an overshoot of the desired operating temperature. At steady state conditions the model matches experimental data. The difference in overshoot temperature is 4.5°C, or 7%. Experimental data show the system reaching the peak overshoot temperature at 2134 seconds. The simulation reaches the peak overshoot at 2974 seconds, 39% longer. The experimental data show the air temperature rebounding to -26.4°C before finally dropping to a steady state vale of -29°C. The simulation gives a rebound temperature of -27.0°C before it reaches steady state at -29°C.

Experimental and Simulated Air Temperature

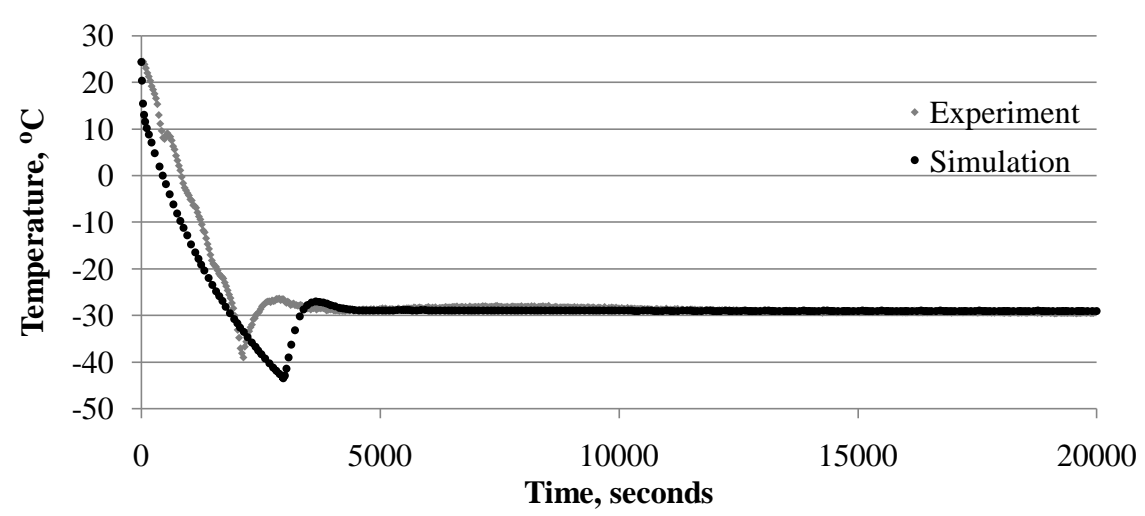


Figure 12. Simulated freezer air temperature matches the steady state experimental values and captures the qualitative transient behavior

The initial bow of the model is attributed to a difference in predicted heat transfer rate. The model uses an initial value of 100 (W). In reality, the system first receives a burst of warm nitrogen gas. Then cooler nitrogen gas moves its way through the supply tube. As the tube cools down, LN₂ can begin to propagate towards the valve. This process takes a certain amount of time which the model does not take into account.

The simulation of the bulb temperature is accurate at steady state and predicts qualitative transient behavior well (Fig. 13). This is not surprising as the bulb model was built for steady state conditions like the chest model. The simulation results suggest that the model predicts a longer bulb time constant than the actual time constant.

Experimental and Simulated Bulb Temperature

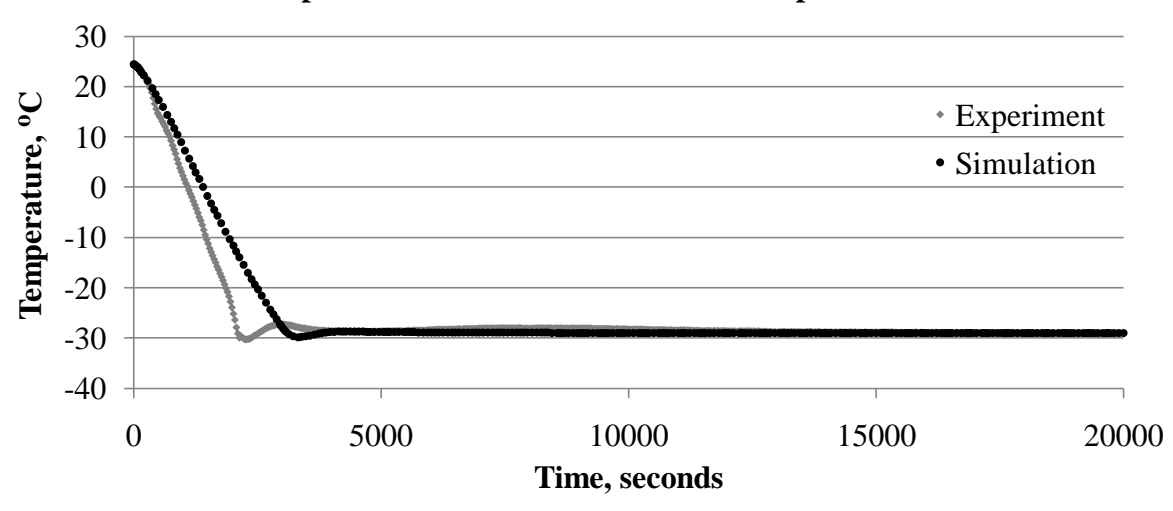


Figure 13. The simulated sensor bulb temperature decreases slower than experimental measurements but matches the steady state values.

The simulation also predicts the heat transfer rate \dot{Q}_{LN2} (Fig. 14). The cooling function starts out in saturation at 100 (W). Once the bulb temperature reaches the operating point \dot{Q}_{LN2} drops off dramatically as the air temperature overshoots the operating point. The steady state value of \dot{Q}_{LN2} is 39 (W). This matches qualitative behavior of valve as well as the steady state

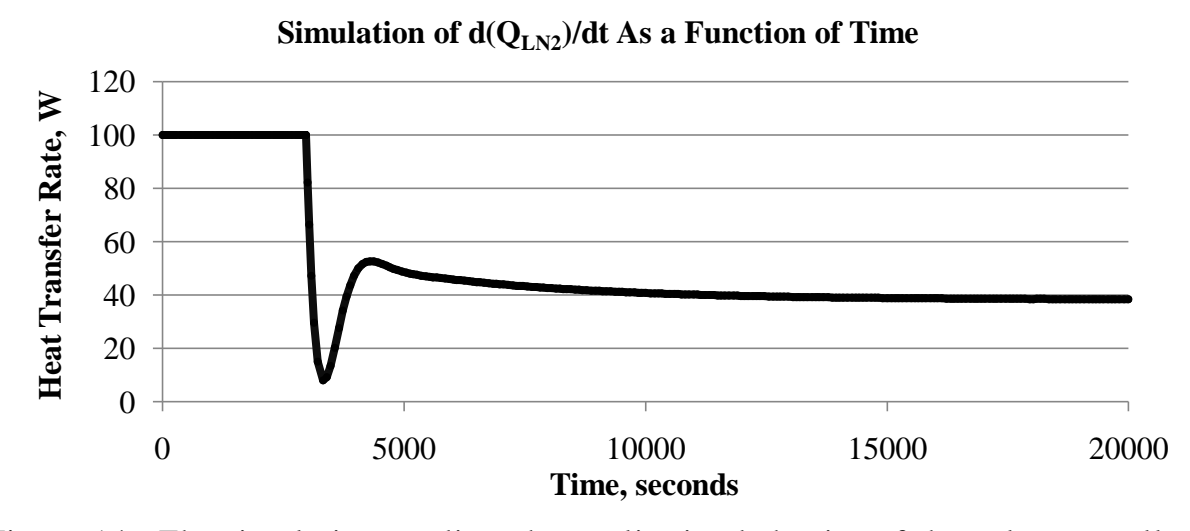


Figure 14. The simulation predicts the qualitative behavior of the valve as well as the correct steady state heat transfer rate.

heat transfer rate.

Alterations to the model can be made to produce quantitatively more accurate simulation results during the transient. Three parameters that can be changed are τ_{bulb} , \dot{Q}_{LN2}^{sat} , and the heat capacities of the freezer components. The transient time can be shortened by decreasing τ_{bulb} to 360 seconds and increasing \dot{Q}_{LN2}^{sat} to 180 (W). By increasing each freezer chest component's heat capacity by a factor of 1.75 the overshoot is controlled. While these alterations change the transient behavior of the model, the steady state results to do not significantly change. The alterations were made in an iterative process to better fit the experimental data.

Experimental Data and Altered Model Simulation

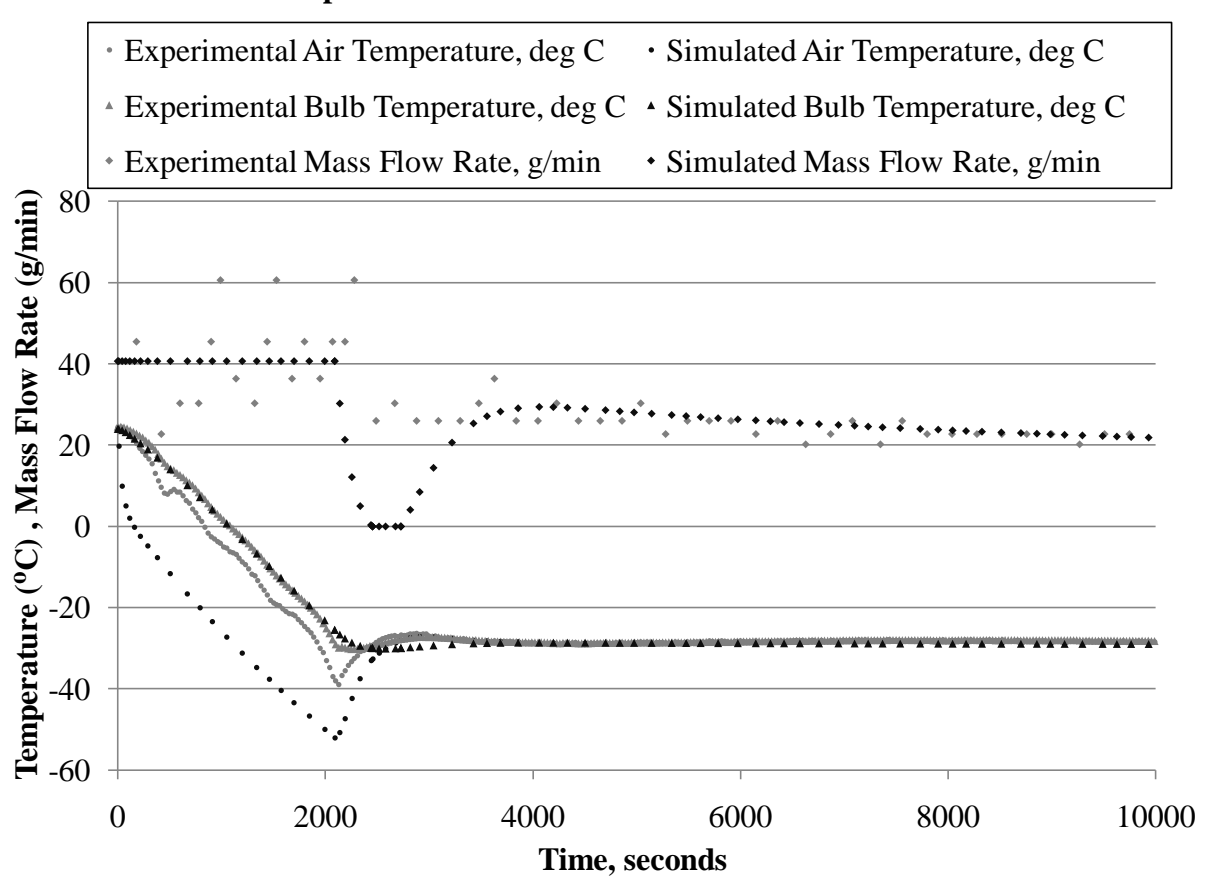


Figure 15. Timing and overshoot is improved with alterations to the model while steady state behavior is not significantly changed.

The simulation of the altered model yields results that closely match the experimental data (Fig. 15). The simulated air temperature still decreases too quickly, however after about 160 seconds its slope closely resembles the experimental measurements. The simulated peak overshoot is 22% more than experimental measurements, although the model predicts accurately the time at which the peak overshoot occurs. This time matches the time at which the flow of LN₂ begins to be decrease. As the bulb temperature drops below the set point, the flow of LN₂ quickly stops. The flow of LN₂ increases to its steady state value once the bulb temperature rises to its steady state value.

The simulated mass flow rate of LN₂ is calculated by dividing the simulated heat transfer rate by the specific heat transfer of nitrogen. It is assumed that there is 50% quality flow during the transient. It was observed that during the transient there was two-phase flow of nitrogen through the TEV and that about half of the LN₂ boils before reaching the TEV. The specific heat transfer for 50% quality flow is 265,500 (J/kg). At steady state it was observed that only gas phase nitrogen exits the TEV. A pure gas phase flow has a specific heat transfer of 113,200 (J/kg). The specific heat transfer for the corresponding quality of flow was used to calculate the transient and steady state mass flow rates. The simulated \dot{m}_{LN2} matches very well with averaged experimental measurements.

The model can be used to predict the system response to a power failure and a dramatic increase in room temperature (Fig. 16). The simulation assumes excellent insulation of the LN₂ supply tank and supply line such that liquid phase nitrogen is delivered to the chest. The simulation starts with the air temperature at -35°C and the conventional refrigeration system running. The ambient room temperature is 23°C. A power loss occurs causing the refrigeration

Simulated System Response to Complete Power Loss

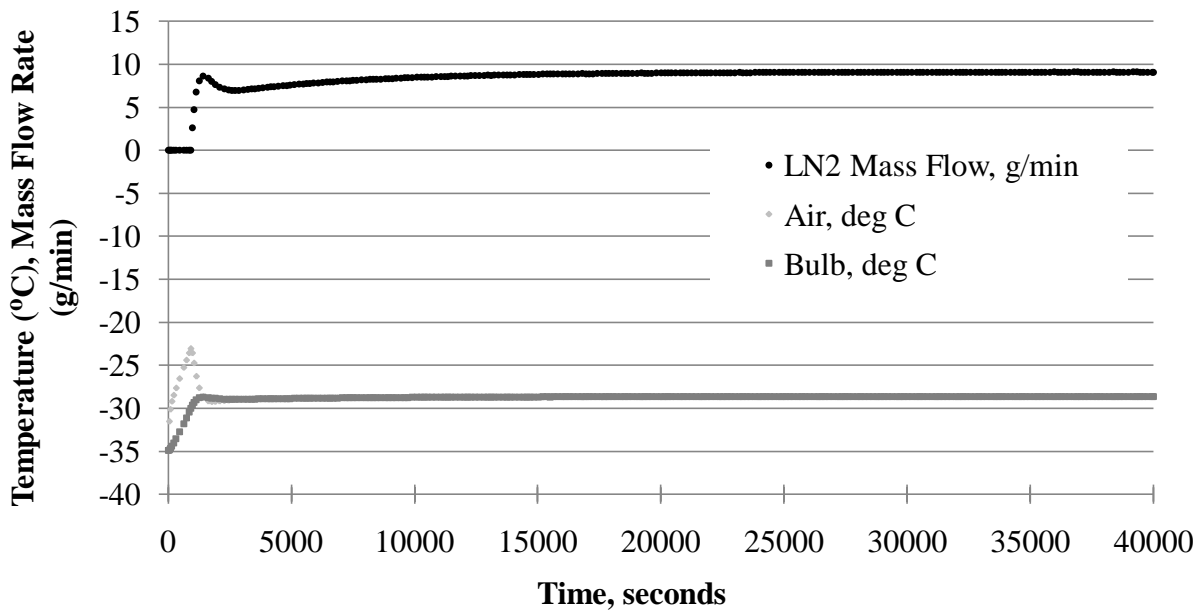


Figure 16. Simulation shows that the LN₂ TEV system is well suited to backup a primary refrigeration system during the worst conditions of a power failure.

system to shut down. In a worst case scenario the room temperature instantly increases to 50°C (122°F). After about 12 minutes the bulb temperature rises above the set point and triggers the flow of LN₂. At this point the air temperature has risen to -23°C. However, it is known that the simulation overshoots by 22% more than experimental data which suggests that the air temperature would rise no higher than -25°C. The air temperature would reach a steady state temperature of -28.6°C with a mass flow rate of 9.1 (g/min) corresponding to a heat transfer rate of 55 (W). The simulation shows that the LN₂ TEV system quickly regulates the freezer temperature. If the power failure lasts 7 days, the mass flow rate of 9.1 (g/min) corresponding to 30 gallons of LN₂, costs \$6. This an extremely low cost for the value of the biological material being preserved.

The simulation is a worst case scenario. When power loss occurs, the room temperature would not instantly rise to the outside temperature. Also the chest is assumed to be empty. If the

chest were full the freezer heat capacity would increase greatly. The higher heat capacity and the gradual rise in room temperature would result in a very slow increase in freezer air temperature. The increased time constant of the freezer would be many times longer than the bulb time constant so there would be little or no overshoot of the set point temperature.

CONCLUSION

Experimental results of the LN_2 TEV indicate successful operation. The steady state freezer air temperature was regulated to within 1° C of the LN_2 TEV set point of -30° C. Mass flow rate measurements show proper actuation of valve motion as the flow rate dropped to a steady value as the air temperature reached its steady state value. Increased steady state mass flow rate and temperature overshoot in the transient were the result of a poorly insulated, small commercial LN_2 supply tank and an empty freezer chest. The tank was incapable of supplying the TEV with liquid N_2 during the low steady state flow rates because the liquid would boil upon reaching the top of the tank. A chest full of biological material would reduce or eliminate overshoot because of the great increase in heat capacity of the freezer. However, these issues do not affect the functionality of the LN_2 TEV.

Mathematical models were developed to describe system behavior and estimate system parameters. Simulation of the model predicted qualitative transient behavior, as well as peak overshoot timing and steady state temperatures and mass flow rates that matched experimental data. Simulation of a refrigeration power loss and ambient temperature rise situation shows that the LN₂ TEV is capable of quickly regulating freezer air temperature. This is due to the LN₂ TEV's high gain and reserve cooling capacity at steady state.

Further work on the LN_2 TEV should involve testing with proper insulation and tubing as well as different TEV refrigerant charges. Vacuum insulated tubing and proper tank insulation would better simulate a commercial application of the LN_2 TEV. Different refrigerant charges would change the operating temperature. One could be used in a backup system for a -86°C freezer, a common cryogenic appliance. Though the operating temperature set point changes

with bulb refrigerant charge, the valve would function in the same way as was experienced in experiments and described by the mathematical model.

The LN₂ TEV backup refrigeration system meets the need for a more reliable backup refrigeration system for the long term storage of biological material. A common TEV was modified to be used with LN₂ by improving an important seal and insulating the valve actuator. The TEV operates without the use of an external energy source as it converts its own thermodynamic energy into mechanical movement. The LN₂ TEV system is capable of operating in the presence of water with the cold and pressurized chest able to seal leaks in water up to 50ft deep. The only external requirement for the system is a large LN₂ source which is common in facilities that store biological material. Use of the LN₂ TEV backup refrigeration system in research and storage facilities could save thousands of biological samples, worth millions of dollars and years of research, from future natural disasters.

APPENDICES

APPENDIX A: THERMAL INSULATION CALCULATIONS

Material properties were taken from [Incropera et al., 2007] and [Callister, 2007]. The conduction heat transfer rate from the diaphragm to the valve body

$$\dot{Q}_{conduction} = [(k \times A_c)/L] \times (T_D - T_V) \tag{A-1}$$

where k is the thermal conductivity of the polycarbonate extension, A_c is the cross-sectional area, L is the extension length, T_D is the diaphragm temperature, and T_V is the valve body temperature. The convection heat transfer rate from the freezer air to the midpoint of the extension

$$\dot{Q}_{convection} = (h \times A_H) \times [T_A - (T_D + T_V)/2] \tag{A-2}$$

where h is the convection heat transfer coefficient, A_H is the extension surface area, and T_A is the freezer air temperature. Setting (A-1) and (A-2)) equal to each other and solving for L

$$L^{2} = kA_{c}(T_{D} - T_{V})/h\pi D[T_{A} - (T_{D} + T_{V})/2]$$
(A-3)

Inserting property values, dimensions, and temperatures yields

$$L^{2} = \frac{0.2 (W/m \cdot K) \times 0.00018 (m \cdot m) \times [-100 (^{o}C) + 196 (^{o}C)]}{3 (W/m \cdot m \cdot K) \times 0.06 (m) \times [-30 (^{o}C) + 148 (^{o}C)]}$$
(A-4)

Carrying out the calculation and double the length for a factor of safety for 2

$$L = 2.6 \times 10^{-2} \,(m) \tag{A-5}$$

The extension rod of length 2.6 cm must be able to handle the forces exerted on it by the diaphragm and spring without buckling. The maximum force that can be placed on the rod without buckling $P = \pi^2 EI/(0.65L)^2$,

$$P = \pi^{2}[2.38 (GPa)][4.99x10^{-12}(m^{4})]/[0.65 \times 2.6x10^{-2}(m)]^{2}$$

$$= 410 (N)$$
(A-6)

APPENDIX B: RESISTANCE AND HEAT CAPACITY CALCULATIONS

Material properties were taken from [Incropera et al., 2007] and [Callister, 2007].

INTERIOR (properties evaluated at 250K)

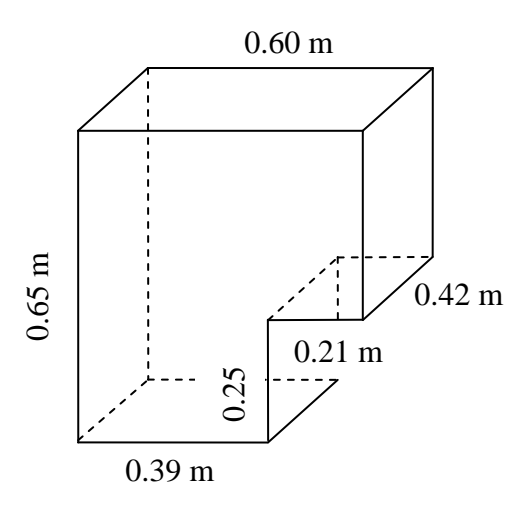


Figure 17. Chest interior dimensions.

Area

Aluminum sides and bottom:

 $[(0.65 \text{ m x } 0.39 \text{ m}) + (0.21 \text{ m x } 0.40 \text{ m})] \text{ x } 2 = 0.66 \text{ m}^2$

 $(0.65 \text{ m x } 0.42 \text{ m}) \text{ x } 2 = 0.54 \text{ m}^2$

 $(0.60 \text{ m x } 0.42 \text{ m}) \text{ x } 1 = 0.25 \text{ m}^2$

Aluminum Total = 1.45 m^2

Polystyrene top:

 $(0.60 \text{ m x } 0.42 \text{ m}) \text{ x } 1 = 0.25 \text{ m}^2$

Total Interior Area: 1.70 m²

Resistance

 $R_{al} = 7.5 \times 10^{-4} \text{ m/} (170 \text{ W/m-K} \times 1.45 \text{ m}^2) = 3.0 \times 10^{-6} \text{ K/W}$

$$R_{ps} = 7.5 \times 10^{-4} \text{ m/} (0.13 \text{ W/m-K} \times 0.25 \text{ m}^2) = 2.3 \times 10^{-2} \text{ K/W}$$

$$R_{int_wall} = (R_{al}^{-1} + R_{ps}^{-1})^{-1} = 3.0x10^{-6} \text{ K/W}$$

Volume

Aluminum : $1.45 \text{ m}^2 \text{ x } 7.5 \text{x} 10^{-4} \text{ m} = 1.1 \text{x} 10^{-3} \text{ m}^3$

Polystyrene : $0.25 \text{ m}^2 \text{ x } 7.5 \text{ x} 10^{-4} \text{ m} = 1.9 \text{ x} 10^{-4} \text{ m}^3$

Total: $1.3x10^{-3}$ m³

Heat Capacity

$$C_{al} = (1.1 \times 10^{-3} \text{ m}^3)(2770 \text{ kg/m}^3)(830 \text{ J/kg-K}) = 2.5 \times 10^3 \text{ J/K}$$

$$C_{ps} = (1.9x10^{-4} \text{ m}^3)(1050 \text{ kg/m}^3)(1170 \text{ J/kg-K}) = 2.3x10^2 \text{ J/K}$$

$$C_{int} = C_{al} + C_{ps} = 2.7x10^3 \, J/K$$

EXTERIOR (aluminum)

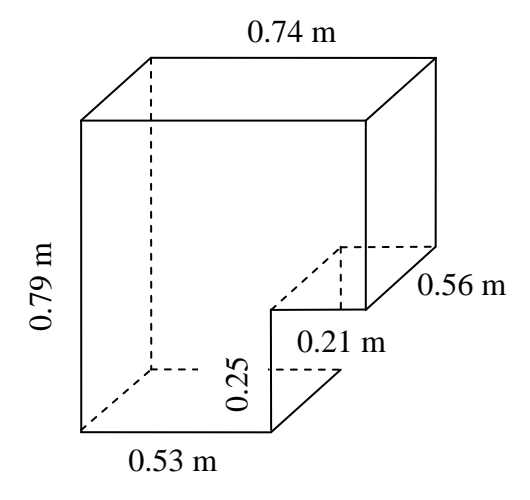


Figure 18 Chest exterior dimensions.

<u>Area</u>

$$(0.79 \text{ m x } 0.53 \text{ m}) \text{ x } 2 = 0.84 \text{ m}^2$$

$$(0.54 \text{ m x } 0.21 \text{ m}) \text{ x } 2 = 0.22 \text{ m}^2$$

$$(0.74 \text{ m x } 0.56 \text{ m}) \text{ x } 2 = 0.82 \text{ m}^2$$

$$(0.79 \text{ m x } 0.56 \text{ m}) \text{ x } 2 = 0.88 \text{ m}^2$$

Total Exterior Area = 2.76 m^2

Resistance

$$R_{ext_wall} = 7.5 \times 10^{-4} \text{ m/} (176 \text{ W/m-K} \times 2.76 \text{ m}^2) = 1.5 \times 10^{-6} \text{ K/W}$$

Volume

$$V_{ext} = 2.76 \text{ m}^2 \text{ x } 7.5 \text{x} 10^{-4} \text{ m} = 2.1 \text{x} 10^{-3} \text{ m}^3$$

Heat Capacity

$$C_{\text{ext}} = (2.1 \text{x} 10^{-3} \text{ m}^3)(2770 \text{ kg/m}^3)(871 \text{ J/kg-K}) = 5.1 \text{x} 10^3 \text{ J/K}$$

INSULATION (urethane foam)

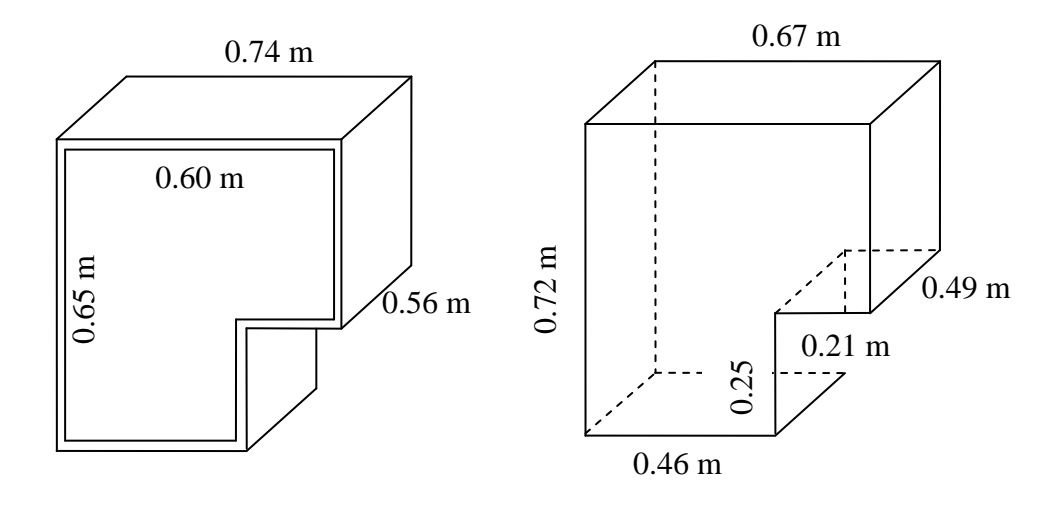


Figure 19. Chest insulation dimensions.

Area

$$(0.72 \text{ m x } 0.46 \text{ m}) \text{ x } 2 = 0.66 \text{ m}^2$$

$$(0.47 \text{ m x } 0.21 \text{ m}) \text{ x } 2 = 0.198 \text{ m}^2$$

 $(0.67 \text{ m x } 0.49 \text{ m}) \text{ x } 2 = 0.66 \text{ m}^2$

 $(0.72 \text{ m x } 0.49 \text{ m}) \text{ x } 2 = 0.70 \text{ m}^2$

Total Insulation Area = 2.22 m^2

Resistance

$$R_{ins} = 7.0 \times 10^{-2} \text{ m/} (0.026 \text{ W/m-K} \times 2.22 \text{ m}^2) = 1.2 \text{ K/W}$$

Volume

Sides, top and bottom:

$$0.56 \text{ m x} [(0.79 \text{ m x } 0.74 \text{ m}) - (0.65 \text{ m x } 0.60 \text{ m})] = 0.11 \text{ m}^3$$

Front and back: using result from interior area calculation

$$0.66 \text{ m}^2 \text{ x } 7 \text{x} 10^{-2} \text{ m} = 0.05 \text{ m}^3$$

$$V_{ins} = 0.16 \text{ m}^3$$

Heat Capacity

$$C_{ins} = (0.16 \text{ m}^3)(70 \text{ kg/m}^3)(1045 \text{ J/kg-K}) = 1.2 \text{x} 10^4 \text{ J/K}$$

<u>AIR</u>

Volume

Using area result from interior front and back panel area calculation

$$V_{air} = 0.33 \text{ m}^2 \text{ x } 0.42 \text{ m} = 0.14 \text{ m}^3$$

Heat Capacity

$$C_{air} = (0.14 \text{ m}^3)(1.4354 \text{ kg/m}^3)(1006 \text{ J/kg-K}) = 2.0 \text{x} 10^2 \text{ J/K}$$

SUMMARY

Table 5. Resistance and heat capacity summary

Component	Thermal Resistance R (K/W)	Heat Capacity C (J/K)
Air	_	2.0×10^2
Interior	0.12	2.7×10^3
Insulation	1.2	1.2×10^4
Exterior	0.018	5.1×10^3

APPENDIX C: SENSOR BULB HEAT TRANSFER

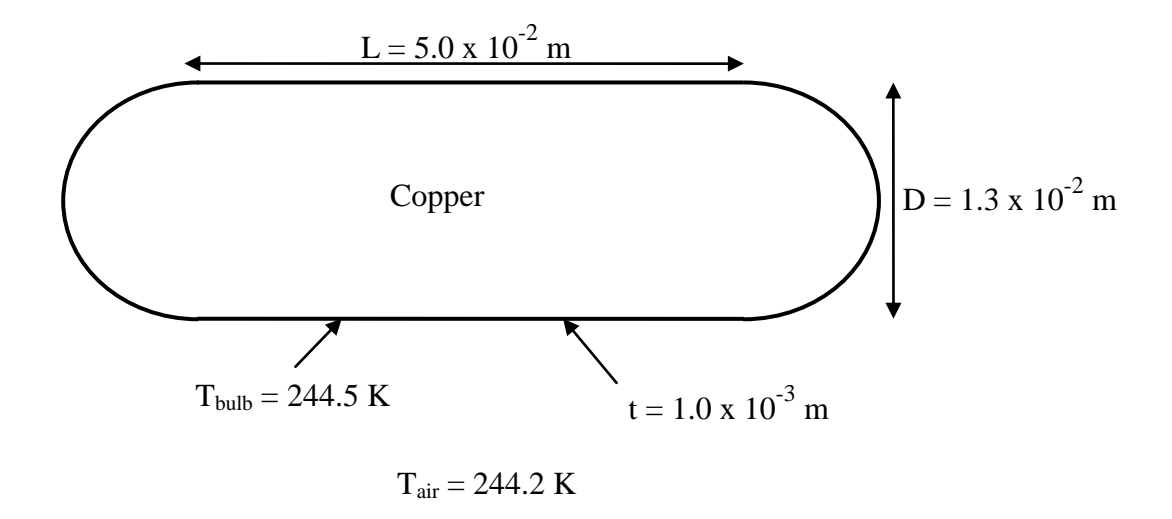


Figure 20. Sensor bulb geometry.

Conservation of energy is used to model the heat transfer from the freezer air at temperature T_{air} to the sensor bulb at temperature T_{bulb} (C-1). The time rate of change of energy in the bulb \dot{E}_{bulb} is equal to the heat transfer rate into the bulb \dot{Q} .

$$\dot{E}_{bulb} = \dot{Q} \tag{C-1}$$

The change in energy stored in the bulb is equal to the product of the bulb's heat capacitance C_{bulb} and the time rate of change of the bulb's temperature \dot{T}_{bulb} (C-2). The heat transfer rate into the bulb is equal to the temperature difference between the air and bulb divided by the thermal resistance R.

$$C_{bulb}\dot{T}_{bulb} = (1/R)(T_{air} - T_{bulb}) \tag{C-2}$$

The calculation of the heat capacitance of the bulb C_{bulb} is begun by calculating the surface area of the bulb (C-3). The total surface area is approximated as the surface area of a cylinder and a sphere.

$$A = \pi DL + \pi D^2 = \pi (1.3x10^{-2}m)(5.0x10^{-2}m) + \pi (1.3x10^{-2}m)^2$$
$$= 2.5x10^{-3}m^2$$
(C-3)

Next the volume is calculated by multiplying the surface area by the thickness of the bulb's wall (C-4).

$$V = A \cdot t = 2.5x10^{-3}m^2 \cdot 1.0x10^{-3}m = 2.5x10^{-6}m^3$$
 (C-4)

The mass of the bulb is the product of the volume and density (Table 6) of the copper bulb (C-5).

Table 6. Material properties of copper at 244.5 K [Incropera et al., 2007]

Density ρ (kg/m ³)	Specific Heat c (J/kg-K)
8933	369

$$m = V \cdot \rho = 2.5x10^{-6}m^3 \cdot 8933(kg/m^3) = 2.2x10^{-2}kg$$
 (C-5)

Finally, the heat capacitance of the bulb is product of the bulb mass and the specific heat (C-6).

$$C_{bulb} = m \cdot c_p = 2.2x \cdot 10^{-2} kg \cdot 369 (J/kg \cdot K) = 8.1 (J/K)$$
 (C-6)

The thermal resistance R between T_{air} and T_{bulb} is equal to the product of the convection heat transfer coefficient and bulb area. The process of calculating the convection heat transfer coefficient h starts with calculating the Raleigh number Ra_D (C-7) using properties of air (Table 7) [Incopera et al., 2007].

Table 7. Thermal properties of air at 244.2 K [Incropera et al., 2007]

Density ρ (kg/m ³)	Kinematic Viscosity v (m ² /s)	Thermal Conductivity <i>k</i> (W/m-K)	Thermal Diffusivity $\alpha \text{ (m}^2\text{/s)}$	Prandtl Number Pr	Thermal Expansion Coefficient β (K^{-1})
1.4354	10.99x10 ⁻⁶	21.8×10^{-3}	15.3×10^{-6}	0.722	$4.0x10^{-3}$

$$Ra_D = g\beta (T_{bulb} - T_{air})D^3/v\alpha = 150$$
 (C-7)

The Raleigh number is used in the calculation of the Nusselt number \overline{Nu}_D using the correlation for a horizontal cylinder under natural convection (C-8) [Incropera et al., 2007].

$$\overline{Nu}_D = \left\{ 0.60 + \left(0.378 \, Ra_D^{1/6} \right) / \left[1 + \left(0.559 / Pr \right)^{9/16} \right]^{8/27} \right\}^2 = 1.8 \quad \text{(C-8)}$$

The convection heat transfer coefficient is directly calculated using the Nusselt number (C-9).

$$h = k\overline{Nu}_D/D = 3.0 \tag{C-9}$$

The thermal resistance is calculated using the convection heat transfer coefficient and the surface area of the bulb (C-10).

$$R = 1/(h \cdot A) = 130(K/W)$$
 (C-10)

The differential equation (C-11) describing the time rate of change of the sensor bulb's temperature comes from rearranging (C-2).

$$\dot{T}_{hulh} = -(1/RC_{hulh})T_{hulh} + (1/RC_{hulh})T_{air}$$
 (C-11)

The time constant of the bulb τ_{bulb} is equal to the product of the thermal resistance and the bulb's heat capacity (C-12).

$$\tau_{bulb} = R \cdot C_{bulb} = 1100 s \tag{C-12}$$

APPENDIX D: HEAT TRANSFER RATES CALCULATION

Material properties were taken from [Incropera et al., 2007] and [Callister, 2007].

Steady State:

The steady state heat transfer rate into the freezer is equal to the temperature difference between the exterior of the freezer wall and the interior of the freezer wall divided by the total thermal resistance of the freezer wall.

$$\dot{Q}_{ss} = (T_{ext} - T_{int}) / \left(R_{int_wall} + R_{ins} + R_{ext_wall}\right)$$

$$\dot{Q}_{ss} = (295.4K - 248.7K) / \left(3.0x10^{-6} \frac{K}{W} + 1.2 \frac{K}{W} + 1.5x10^{-6} \frac{K}{W}\right) = 39 W$$

The steady state heat transfer rate out of the freezer from the heat absorbed by the temperature change of the nitrogen gas is equal to the product of the specific heat transfer rate of nitrogen and the mass flow rate of nitrogen.

The two heat transfer rates are extremely close as expected for steady state conditions.

Saturation:

The linear nature of the temperature drop of the air implies a constant heat transfer rate. The TEV is a proportional controller but includes saturation due to maximum and minimum orifice

areas. The minimum heat transfer rate is 0 (W) when the valve is closed. The slope of the Air Temperature line will determine the maximum heat transfer rate. The slope is determined from the points (1 min, 23.85 °C) and (33.5 min, -33.08 °C) (Table 8).

$$\dot{T}_{air} = \frac{1}{C_{air}} \left[\frac{1}{R_{int}} (T_{int} - T_{air}) - \dot{Q}_{LN2} \right]$$

$$\dot{Q}_{LN2}^{Sat} = -C_{air}\dot{T}_{air} + \frac{1}{R_{int}}(T_{int} - T_{air})$$

Table 8. Thermal parameters used in the transient heat transfer rate calculation

$C_{air}, (J/K)$	$\dot{T}_{air}, (J/s)$	R_{int} , (K/W)	Avg. $(T_{int} - T_{air})$, (K)
2.0×10^2	-2.9×10^{-2}	0.12	12

$$\dot{Q}_{LN2}^{Sat} = (-) \ 2.0x 10^{2} \frac{J}{K} \times -2.9 \ x \ 10^{-2} \frac{K}{s} + \frac{1}{0.12 \frac{K}{W}} \times 12K = 100W$$

REFERENCES

REFERENCES

Air Liquide, 2009, "Gas Encyclopaedia", Air Liquide Group, Paris, France http://encyclopedia.airliquide.com/Encyclopedia.asp?GasID=141

Associated Press, 2005, "Katrina floods wipe out years of research", MSNBC, September 14, http://www.msnbc.msn.com/id/9339191/.

Broersen, P.M.T., 1982, "Control with a thermostatic expansion valve", *International Journal of Refrigeration*, Vol. 5, No. 4, July, pp. 209-212, Butterworth and Co. (Publishers), Ltd., London, England.

Callister, W.D., Jr., 2007, *Materials Science and Engineering an Introduction* (7th ed), pp. A5-A26, John Wiley & Sons, Inc., Hoboken, NJ.

Incropera, F.P., DeWitt, D.P., Bergman, T.L., and Lavine, A.S., 2007, *Introduction to Heat Transfer* (5th ed), pp. 840-855, John Wiley & Sons, Inc., Hoboken, NJ.

Institute for Health Care Studies, 2010, "ICHS Brochure", College of Human Medicine, Michigan State University, http://ihcs.msu.edu/pdf/IHCSBrochure_000.pdf.

Moran, M.J. and Shapiro, H.N., 2004, *Fundamentals of Engineering Thermodynamics* (5th ed), pg. 592, John Wiley & Sons, Inc., Hoboken, NJ.

Parker Hannifin Corporation, 2007, "Thermostatic and Automatic Expansion Valves, Catalog E-1", Parker Hannifin Corporation Climate and Industrial Controls Group, Cleveland, OH, October.

Radcliffe, C., 2007, "Liquid Nitrogen (LN2) and How It Works", Presentation to Biorepository Research Group, Michigan State University, East Lansing, MI, March 2.

Radermacher, R., Yang, B., and Hwang, Y., 2007, "Integrating Alternative And Conventional Cooling Technologies", *ASHRAE Journal*, October, American Society of Heating, Refrigerating and Air-Conditioning Engineers, Inc., pp. 28-35.

Reynolds, W.C., 1979, *Thermodynamic Properties in SI*, pp. 54-55, Department of Mechanical Engineering, Stanford University, Stanford, CA.

Sanyo, 2010, "Status Alert Functions for Ultra Low Freezers", SANYO Biomedical and Environmental Solutions, Wood Dale, IL, http://us.sanyo.com/Dynamic/customPages/docs/biomedical_TechBulletinVIPStatusAlert.pdf.

Turner, A., Teachey, L., Berger, E., Snyder, M., Nissimov, R., Dawson, B., Markley, M., Garcia, M., Ackerman, T., Hegstrom, E., Olafson, S., and Kliewer, T., 2001, "The Great Flood of 2001",

The Houston Chronicle, Houston Chronicle Publishing Company Division, Houston, TX, June 12.

U.S. Energy Information Administration, 2010, "Average Retail Price of Electricity to Ultimate Customers by End-Use Sector, by State", *Electric Power Monthly*, November, http://www.eia.doe.gov/electricity/epm/table5_6_b.html